

# Hybrid three-dimensional (3D) bioprinting of retina equivalent for ocular research

Pujiang Shi<sup>1</sup>, Tan Yong Sheng Edgar<sup>1</sup>, Wai Yee Yeong<sup>1\*</sup> and Augustinus Laude<sup>2</sup>

<sup>1</sup> Singapore Centre for 3D Printing, School of Mechanical and Aerospace Engineering, Nanyang Technological University, 50 Nanyang Avenue Singapore 639798

<sup>2</sup> National Healthcare Group Eye Institute, Tan Tock Seng Hospital, Singapore 308433

**Abstract:** In this article, a hybrid retina construct was created via three-dimensional (3D) bioprinting technology. The construct was composed of a PCL ultrathin membrane, ARPE-19 cell monolayer and Y79 cell-laden alginate/pluronic bioink. 3D bioprinting technology was applied herein to deliver the ARPE-19 cells and Y79 cell-laden bioink to ensure homogeneous ARPE-19 cell seeding; subsequently, two distinctive Y79 cell-seeding patterns were bioprinted on top of the ARPE-19 cell monolayer. The bioprinted ARPE-19 cells were evaluated by prestoblue assay, F-actin, and hematoxylin/eosin (HE) staining, and then the cells were observed under laser scanning and invert microscopy for 14 days. The Y79 cells in alginate/pluronic bioink after bioprinting had been closely monitored for 7 days. Live/dead assay and scanning electrical microscopy (SEM) were employed to investigate Y79 cell viability and morphology. Both the ARPE-19 and Y79 cells were in excellent condition, and the successfully bioprinted retina model could be utilized in drug delivery, disease mechanism and treatment method discoveries.

**Keywords:** retina, bioprinting, age-related macular degeneration, tissue engineering

\*Correspondence to: Wai Yee Yeong, Singapore Centre for 3D Printing, School of Mechanical and Aerospace Engineering, Nanyang Technological University, 50 Nanyang Avenue Singapore 639798, Singapore; Email: WYYeong@ntu.edu.sg

**Received:** June 26, 2017; **Accepted:** July 3, 2017; **Published Online:** July 10, 2017

**Citation:** Shi P, Edgar T Y S, Yeong W Y, *et al.*, 2017, Hybrid three-dimensional (3D) bioprinting of retina equivalent for ocular research. *International Journal of Bioprinting*, vol.3(2): 138–146. <http://dx.doi.org/10.18063/IJB.2017.02.008>.

## 1. Introduction

The retina is a complex multilayered tissue that collects and decrypts information of light energy and then transmits such information to brain to reflect images of the visual environment. Retinal pigment epithelium (RPE) is a highly specialized cell monolayer with pigmented microvilli aligning the Bruch's membrane located between the neural retina and the choroid in the eye<sup>[1]</sup>. Mature RPE cells are mitotically quiescent under the physiological condition in the eyes; however, the RPE cells start to proliferate when the neural retina suffers from traumatic injuries<sup>[1]</sup>. Many retinal diseases may be linked to RPE degeneration. The RPE is an essential supporting tissue for nutrient transport, production of growth factors and phagocytosis of the photoreceptor outer segments<sup>[2]</sup>. The photoreceptor and associated retinal circuitry is a complex system, and it is challenging to be repaired through regenerative medicine<sup>[1,2]</sup>.

Several mechanisms of retina degeneration may cause

outer retina deterioration, including photoreceptors and the associated RPE cells. The degeneration leads to irreversible vision loss, and currently no effective treatments exist to permanently stop the degeneration and to restore normal retinal function from lost vision. There were some reports regarding retinal regeneration, including application of mature photoreceptors, progenitor cells, retinal sheets and RPE cells, and these trials demonstrate improved vision in animal studies. However, the mechanism of the visual improvement is not clear, and the data from animal trial cannot be translated into effective clinical treatments yet. During retinal regeneration, the cell organization/alignment, integration and differentiation into retinal cell types are critical to its functionality. The photoreceptors/RPE complex functional unit is vital for normal vision; furthermore, their layered organization and correct orientation are critical for normal function and survival of the retina. The implanted cells need to complete retinal integration and differentiate into mature retina cell

Hybrid three-dimensional (3D) bioprinting of retina equivalent for ocular research. © 2017 Pujiang Shi, *et al.* This is an Open Access article distributed under the terms of the Creative Commons Attribution-NonCommercial 4.0 International License (<http://creativecommons.org/licenses/by-nc/4.0/>), permitting all non-commercial use, distribution, and reproduction in any medium, provided the original work is properly cited.

types. The implantation of the cells into the subretinal region may cause significant cell loss, and cell behavior after implantation may not be controllable; thus, the implanted retinal cells and tissue may form abnormal rosettes<sup>[3–5]</sup>. Cell viability and differentiation are significantly improved when the cells are transplanted with scaffolds<sup>[6]</sup>.

The scaffolds can provide necessary mechanical and physical supports for cell attachment, proliferation and differentiation<sup>[7,8]</sup>. However, conventional scaffold fabrication methods lack precision, and are incapable to prepare constructs with complex designs<sup>[7,9]</sup>. Three-dimensional (3D) bioprinting can precisely deliver cells and biomolecules to prepare micro-tissues, micro-organs and mimetic extracellular matrix, which bring researchers effective strategies for the investigation of disease progression, drug metabolism and applications of tissue or organ transplantation<sup>[7,10–12]</sup>.

Human retina is a highly complex vascularized tissue that contains at least 60 functionally different cell types, including rod and cone photoreceptor cells, horizontal cells, bipolar cells, amacrine cells, retinal ganglion cells as well as support cells, glial cells, etc.<sup>[1,13]</sup> The multiple cells need to cooperate in concert with each other to successfully relay visual signal to brain, and only specific cells need to be replaced during certain diseases, for example the retinal ganglion cells in glaucoma, or the photoreceptor cells in retinitis pigmentosa<sup>[1,6]</sup>. Moreover, certain areas of the retina may need replacement in some conditions, for example in the treatment of age-related macular degeneration (AMD) that arises as the result of chronic and low-grade inflammation in the central outer retina, leading to the RPE and Bruch's membrane degeneration<sup>[2,14]</sup>. Moreover, there are other diseases that will also cause macular disease<sup>[1,15]</sup>. All the diseases lead to the malfunction of RPE and photoreceptors. In some extreme cases, the whole eyeball may need to be removed and replaced due to retinoblastoma; thus, the 3D bioprinting technology is indeed necessary to regenerate complex retina<sup>[13]</sup>. The retina models are useful for the investigation of neurogenesis regulation and cell diversification for AMD diagnosis and early treatments. There are only few attempts and reports regarding retinal regeneration and *in vitro* retina models. In this paper, the 3D bioprinting technology for creation of RPE (ARPE-19) and photoreceptors (Y79) retina equivalent is reported, and the printed construct may serve as a meaningful retina model for the investigation of RPE and Y79 interactions, and retina-related disease mechanism, treatment options and tissue regenerative strategies.

## 2. Materials and Methods

### 2.1 Materials

Hematoxylin/eosin (HE), chloroform, polyethylene glycol (PEG, Fluka 88276), alginate (W201502), pluronic F-127 (P2443) and calcium chloride were purchased from Sigma-Aldrich. Polycaprolactone (PCL) powder was purchased from Perstorp (Mw 50000). ZO-1 Monoclonal Antibody, FITC (ZO1-1A12), NucBlue® Live ReadyProbes® reagents and ActinGreen™ 488 ReadyProbes® reagents were purchased from Thermo Fisher Scientific.

### 2.2 Cell Culture

Human retinal pigmented epithelial cell line (ARPE-19, CRL-2302; ATCC, Rockville, MD, USA) and human retinoblastoma cell line (Y79, HTB-18™, ATCC) were cultured in DMEM:F12 (ATCC) and RPMI 1640 (ATCC) media at 37 °C with 5% CO<sub>2</sub>, respectively, and the media was supplemented with 10% fetal bovine serum (FBS) and 1% antibiotics.

### 2.3 Bioink Preparation

Alginate and pluronic were exposed and sterilized in INTELLIRAY UV Flood 400, ( $\lambda = 320\text{--}390\text{ nm}$ ; density: 115 mW/cm<sup>2</sup>) for half an hour. 10% alginate solution was prepared by the addition of 10 g of alginate powder in 100 mL double-distilled water, and the solution was incubated in 60 °C overnight. Then, the 10% alginate solution was mixed with pluronic to form a complex bioink consisting of 2% alginate (w/v) and 25% pluronic (w/v). The bioink was stored at 4 °C for future applications.

### 2.4 ARPE-19 Cell Bioprinting

The ARPE-19 cells upon confluence were washed with phosphate-buffered saline (PBS) three times. Then, 2 mL of Trypsin-EDTA (0.25%) was added onto the cells and incubated for 5 mins. When the cells were detached from the flask, the trypsin was neutralized by 5 mL DMEM:F12 full media. The cells were counted and centrifuged, and then they were reconstituted in cell culture media at a concentration of  $1 \times 10^6$  cell/mL. The cell solution was transferred into a cartridge for microvalve-based bioprinting. The bioprinting procedure was based on the drop-by-drop pattern to achieve a final seeding density of  $2,786 \pm 492$  cells/cm<sup>2</sup> on an ultrathin membrane. The ultrathin membrane was fabricated according to our published protocol<sup>[16]</sup>. Then, the cells on the ultrathin membrane were further cultured for two weeks.

## 2.5 Y79 Cell Bioprinting

Y79 cells were in a suspension culture, and the cells were counted before collection. The cell pellet was re-suspended in alginate/pluronic bioink to obtain a final cell density of  $1 \times 10^6$  cell/mL. The Y79 cell-laden bioink was filled in a cartridge and kept at 37 °C. The cartridge was connected to a 21G needle tip, and pressure (2 bars) was applied to motivate the bioink to go through the needle to print two distinctive patterns on the ARPE-19 cell-seeded ultrathin membrane: a high average cell density at the center (HC) and a high average cell density at the periphery (HP). The bioprinted Y79 cell-laden bioink was crosslinked in 50 mmol/L calcium chloride solution for 5 mins. Subsequently, the retina equivalents were cultured in cell culture media.

## 2.6 Bioprinted Retina Equivalent Characterization

The cell viabilities of bioprinted ARPE-19 cells at day 1, 7 and 14 were evaluated by prestoblu (Thermo Fisher, Grand Island, NY, USA) assay in test media (1 mL) consisted of prestoblu (10%) and FBS (5%). Control groups were cells without bioprinting. Then, the cell viabilities were calculated according to vendor's protocol. Meanwhile the bioprinted ARPE-19 cells at day 1, 7 and 14 were fixed in 4% paraformaldehyde; then, they were stained by ActinGreen™ 488 ReadyProbes® and NucBlue® Live ReadyProbes® reagents and observed under inverted microscope (Zeiss). The bioprinted ARPE-19 cells on ultrathin membrane at day 14 were also observed under inverted microscope, and the sample was then fixed by 4% paraformaldehyde and HE stained. The bioprinted samples were stained by ZO-1 Monoclonal Antibody, FITC (ZO1-1A12)/NucBlue® Live ReadyProbes® reagents and ActinGreen™ 488 ReadyProbes®/NucBlue® Live ReadyProbes® reagents and live/dead assay, respectively. The stained samples were observed under inverted microscope (Zeiss) and laser scanning microscope (Zeiss LSM 710). For scanning electron microscope (SEM, JEOL) observation, the samples were fixed at day 1, 7 and 14, and then were dehydrated in 30%, 50%, 75%, 95% and 100% ethanol gradually before critical-point drying, and the samples were sputter-coated (sputtering time 90 s and current 20 mA) by gold before SEM observation.

## 2.7 Statistical Analysis

All data was presented as means  $\pm$  standard deviation ( $n = 3$ ). Statistical analysis was implemented by paired samples *t*-test and multiple comparisons using single-factor analysis of variance (ANOVA) and post-hoc Tukey tests using SPSS Statistics version 19.0, and  $p <$

0.05 was considered statistically significant.

## 3. Results

The whole bioprinting strategies for retinal regeneration could be clearly observed in [Figure 1](#). The bioprinting protocol was designed to precisely and efficiently simulate the biological functions of native retina. The ARPE-19 cells were precisely bioprinted on the ultrathin membrane at discrete places to obtain homogenous cell seeding, and then the cells were allowed to grow for two weeks until the formation of ARPE-19 cell monolayer. The Y79 cell-laden alginate/pluronic bioink were bioprinted on the ARPE-19 cell monolayer to achieve two different cell-seeding densities, as can be seen in [Figure 1 C1 and C2](#). The bioprinted ARPE-19 cells were closely monitored at day 1, 7 and 14 via prestoblu assay ([Figure 2](#)). The trend of cell viability in the bioprinted samples were similar to that of the control, their values increased gradually from day 1 to day 14, and no significant differences were observed in both groups. In [Figure 3](#), the ARPE-19 cell morphology and proliferation were investigated, and the cells attached to the membrane within 24 hours, and then migrated and spread on the membrane. The cell number increased markedly, and finally the bioprinted ARPE-19 cells formed cell monolayer at day 14. The bioprinted ARPE-19 cells on the ultrathin membrane at day 14 were further analyzed by inverted microscope, and the bright field image and HE staining indicated that the bioprinted cells formed an intact cell monolayer on the ultrathin membrane ([Figure 4](#)). The bioprinted ARPE-19 cells on ultrathin membrane were investigated under confocal microscope ([Figure 5](#)). It can be observed that the strong actin filaments were within each cell, and the cells were closely packed with polygonal appearance. Moreover, no cell clusters and aggregations were observed on the ultrathin membrane at week 2. Furthermore, the bioprinted ARPE-19 cells were stained by ZO-1 antibodies ([Figure 6](#)), and it showed that robust tight junctions existed within the ARPE19 cell monolayer.

The Y79 cell-laden alginate/pluronic bioink was printed on the ultrathin membrane upon the formation of ARPE-19 cell monolayer. In [Figure 7](#), the cell-laden bioink was bioprinted into two distinctive patterns: the first one is with the higher average Y79 cell-seeding density at the center, and the other one is the higher average Y79 cell-seeding density at the periphery. The samples in both groups were maintained in culture media for seven days. The Y79 cells in alginate/pluronic bioink after bioprinting were evaluated by live/dead assay, and the live cells were stained in green while dead cells were in red color ([Figure 8](#)). Most of the Y79 cells survived at day 1, and they proliferated obviously at day 4 and 7 with high cell viability. Subsequently, the bioprinted Y79

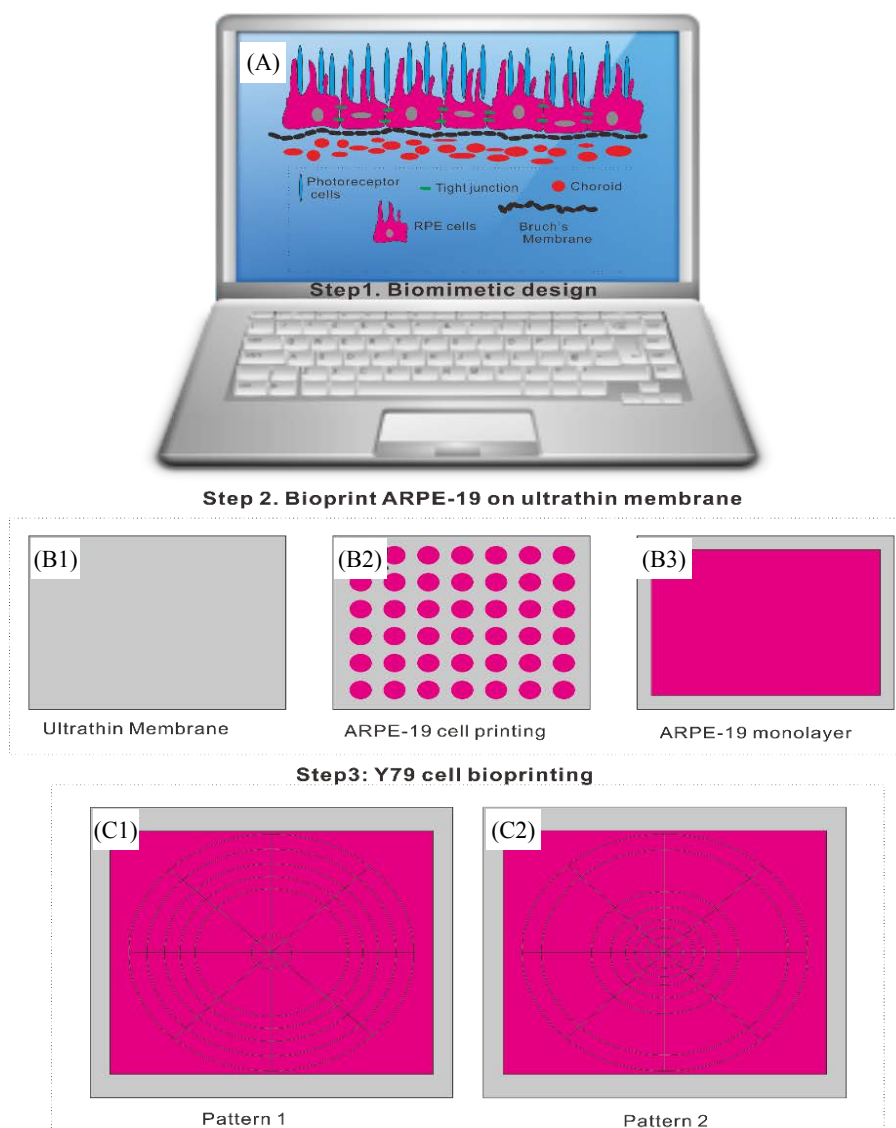


**Figure 1.** Design of bioprinting toolpath for retina equivalent (A); bioprinting of ARPE-19 cells on ultrathin membrane (B1) to obtain homogenous cell seeding (B2) and the cells finally formed monolayer within two weeks (B3); Y79 cell-laden bioink bioprinting toolpath to achieve two distinctive cell-seeding densities: high average cell density at the periphery (HP, C1) and high average cell density at the center (HC, C2).

cell-laden constructs were observed under SEM (Figure 9): the width of each construct was around 0.21 mm, and the smoothly connected constructs maintained consistent morphology in shape and size. The Y79 cells can be observed either at the surface or inside the bioprinted construct (Figure 9D–F), and they were in “sphere” shape.

#### 4. Discussion

Severe retina degeneration due to the malfunction of photoreceptor and RPE cells may finally lead to irreversible vision loss. Current treatment methods can only delay the disease progression, while it is almost

impossible to restore the full function of the deteriorated sensory retina. More importantly, it is challenging to diagnose retina-related diseases at their early stages. For example, AMD is one of the major causes of visual loss in elderly people. 5% of population age above 65 suffers AMD, while the percentage goes up gradually to 12.5% for age 80 and above<sup>[17,18]</sup>. The AMD according to its symptoms can be divided into “dry” and “wet” conditions. Visual loss could happen within months or several years. Majority of AMD initiates as the “dry” type (80%–90% patients), and it may further deteriorate in to “wet” type (10%–20% patients)<sup>[19]</sup>. The early diagnosis of AMD faces many difficulties, and the AMD

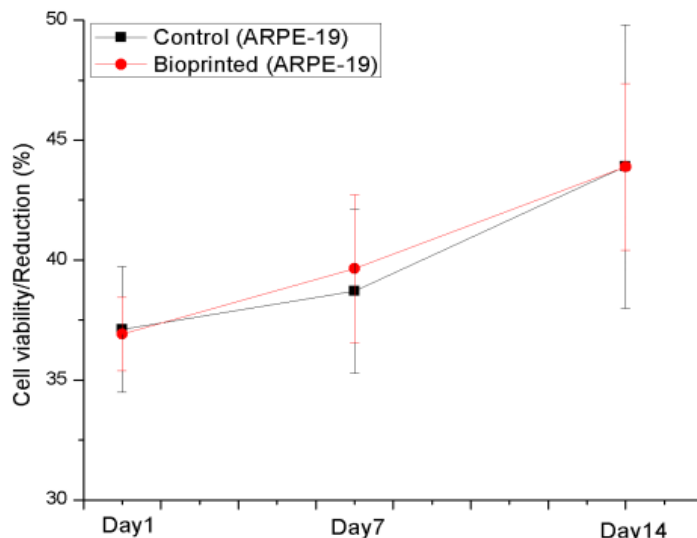


Figure 2. Cell viability assay of manually seeded and bioprinted ARPE-19 cells,  $p > 0.05$

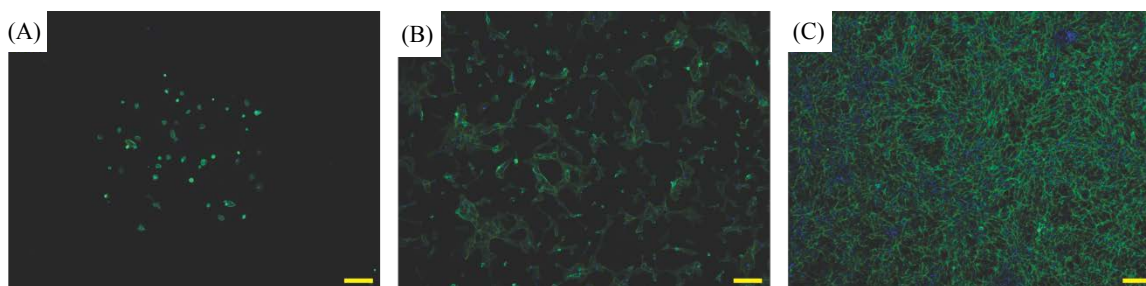


Figure 3. Fluorescent images (F-actin) of bioprinted ARPE-19 cells at day 1 (A), day 7 (B) and day 14 (C); scale bar: 200  $\mu\text{m}$

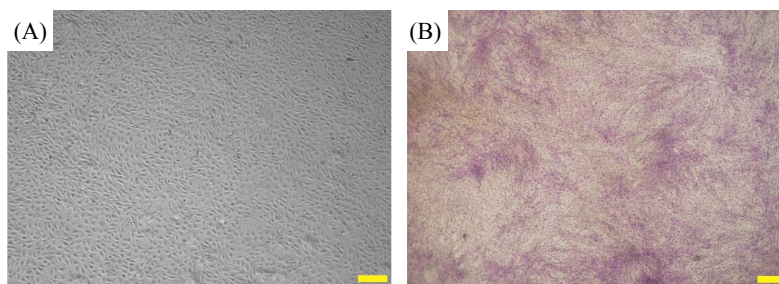
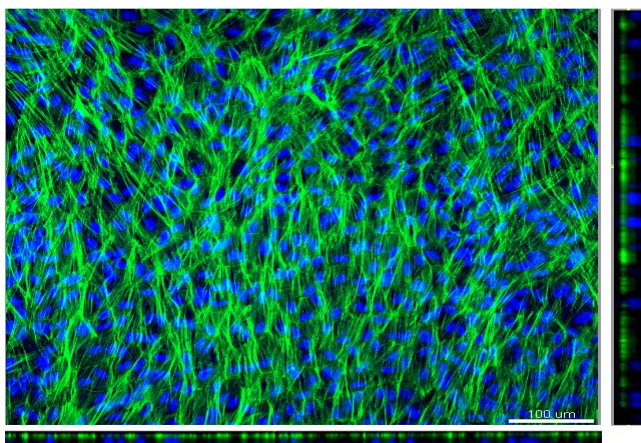


Figure 4. Phase-contrast image of bioprinted ARPE-19 cells on ultrathin membrane (A), and HE staining of bioprinted ARPE-19 cells (B) at week 2; scale bar: 500  $\mu\text{m}$

is usually asymptomatic at its early stages; occasionally some patients experience acute symptoms such as vision loss, unclear vision, scotoma, visual distortion, *etc.*<sup>[20]</sup> The disease development of AMD usually takes long time without symptoms, thus understanding the disease development is largely relative to the wellbeing of the elderly people in the world.

Significant progress in 3D printing technology has demonstrated a potential for organizing advanced cellular and tissue structure with high physiological relevance<sup>[21]</sup>. This technology is successfully applied in many biomedical applications including skin, heart and retina bioprinting, *etc.*<sup>[22]</sup> The 3D bioprinting technology can

efficiently and precisely produce the retina equivalent that a biomimetic platform can be built (Figure 1)<sup>[23–25]</sup>. This proposed platform will be extremely useful for eye-related diseases’ risk assessments and drug testing. In this paper, the ultrathin membrane is utilized to represent Brunch’s membrane, which is a very thin tissue barrier (2–4  $\mu\text{m}$ ) between the retina and choroid. It serves two major roles: as a substratum for metabolically active RPE cell attachment and as a vessel wall. The membrane is involved in AMD and other chorioretinal diseases. The PCL ultrathin membrane enhances cell morphology and barrier formation of ARPE-19 cells, and the stronger and more uniform tight junctions can be observed



**Figure 5.** Confocal images of the bioprinted ARPE-19 cell monolayer on ultrathin membrane; F-actin in green and cell nucleus in blue, with the  $x$ - $y$  projections of single optical section is presented in the central image with respective side-views on  $x$ - $z$  and  $y$ - $z$  (bottom and right) axes; scale bar: 100  $\mu$ m

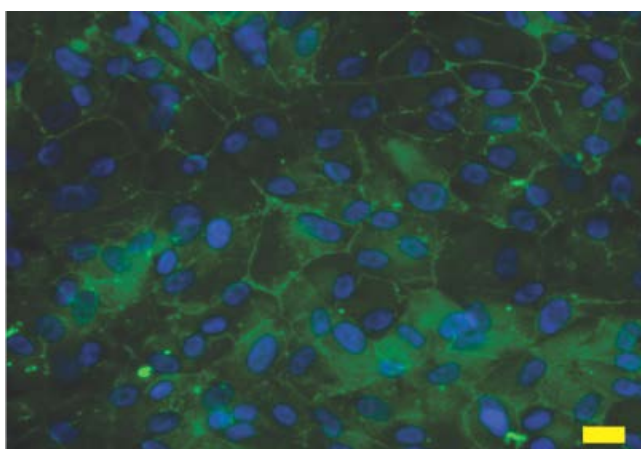


**Figure 6.** ZO-1 and DAPI staining of bioprinted ARPE-19 cell monolayer on ultrathin membrane at week 2; scale bar: 20  $\mu$ m

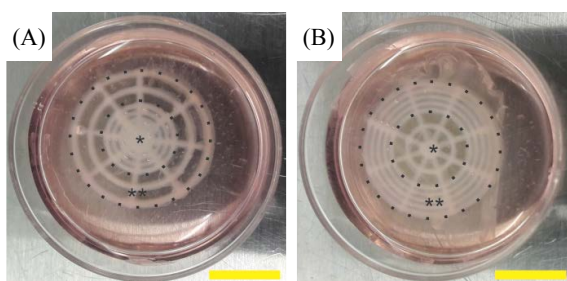


**Figure 7.** The bioprinted retinal equivalents with two distinctive Y79 cell-seeding density: high average cell density at the center (HC, **A**) and high average cell density at the periphery (HP, **B**); \*: central area, \*\*: periphery; scale bar: 10 mm

among ARPE-19 cells on the PCL membrane than that of a transwell membrane<sup>[16]</sup>. The ultrathin membrane is successfully utilized in this research to support ARPE-19 cell seeding, proliferation and formation of monolayer. The bioprinting process does not compromise ARPE-19

cell viability (Figure 2).

The bioprinted ARPE-19 cells show interesting migration patterns on the ultrathin membrane (Figure 3); the cells remain inside the bioprinting droplets at the first 24 hours and subsequently the cells migrate, proliferate and gradually occupy the gap among each droplet, until finally an intact ARPE-19 cell monolayer is formed on the ultrathin membrane. The high quality of ARPE-19 cell monolayer is verified by confocal microscopy and by HE and ZO-1 staining. The cells cover the whole membrane, and no vacant area is observed (Figure 4). In the confocal image, the actin staining indicates intense interactions among cells, while DAPI staining (cell nucleus in blue) proves that no overlaid cells are in the cell layer (Figure 5). Thus, a high quality ARPE-19 cell monolayer is created on the ultrathin membrane.

The vital function of the RPE is to control the ionic composition of the subretinal region, subsequently providing sensory retina the biological environment for its proper function. The sensory retina-related diseases are very subtle and hard to be discovered at their earlier stages; although many scientists prefer to use fresh samples as their experimental model, the available samples are quite limited, especially when they are collected from human<sup>[26]</sup>. On the other hand, animal models may provide alternatives; however, the animal models are not fully controllable and the experimental data is not fully translatable<sup>[27]</sup>. Therefore, cell culture and tissue engineering offer significant flexibility to create *in vitro* retina tissue models and to study the mechanism of retinal regeneration and disease development. The 3D bioprinting technology offers powerful tools for tissue model creation to fully mimic human retina. In this article, the ARPE-19 cell-seeded ultrathin membrane represents Brunch's membrane and RPE monolayer with tight junctions (Figure 6), subsequently the Y79 cell-laden bioink is printed on the APRE-19 cell monolayer to achieve two distinctive patterns (Figure 7). Pure alginate bioink has shown excellent cytocompatibility<sup>[28]</sup>—however the bioink has poor printability. Pluronic is thermoreversible and generally nontoxic, and it has been employed for drug delivery including intramuscular, intraperitoneal and subcutaneous injections<sup>[29]</sup>. Therefore, the alginate/pluronic complex bioink is prepared to maintain excellent biocompatibility and achieve improved printability.

Human photoreceptors are composed of cone and rod cells, and the density distribution of the cone and rod cells are regulated from the foveolar to retinal periphery, with the highest cone concentration is observed at the foveola while rod density is at its maximum density at a 5–6 mm from the foveola<sup>[30]</sup>. Y79 cells express both cone- and rod-specific antigens<sup>[31–33]</sup>, and

fresh retinoblastoma tumor cells can differentiate to photoreceptor, neuronal and glial cell lines<sup>[34]</sup>. Therefore, Y79 cells are useful for retina-related research<sup>[35]</sup> in 3D cell-bioprinting to investigate biological responses of sensory retina cells during and after bioprinting. The bioprinted retina constructs are cultured in media for seven days, and the bioprinted Y79 cell-laden bioink can preserve its basic configuration during the culture period. Although the complex bioink is crosslinked by calcium ions that are slowly released in culture media, its structure may gradually deteriorate. Therefore, the culture media should be carefully and gently removed to avoid structural disruption. The Y79 cell viability is not compromised in the bioink, and the cell density increases from day 1 to day 7 (Figure 8). In SEM images (Figure 9), the Y79 cells can be easily observed on the surface of the bioprinted cell-laden hydrogel; the inner structure of the cell-laden bioink is porous and allows transportation of nutrients and waste, thus providing a benign environment for Y79 cell reproduction while

maintaining biological interactions with the underneath ARPE-19 cell monolayer.

## 5. Conclusion

A retina equivalent was prepared by hybrid 3D bioprinting and reported in this article, and the bioprinted construct was composed of ARPE-19 cell monolayer on ultrathin membrane, and a third layer with two distinctive patterns (Y79 cells in alginate/pluronic bioink). The cell viability, cell morphology and quality of the bioprinted ARPE-19 cells were closely investigated, and the ARPE-19 cells formed high quality monolayer on the ultrathin membrane within 14 days. The Y79 cell-laden alginate/pluronic bioink was successfully bioprinted on the ARPE-19 cell monolayer with two distinctive patterns. The Y79 cells in the bioink showed benign morphology and proliferated in seven days. The bioprinted retina equivalent has acceptable cytocompatibility with advanced structure aiming to simulate native retina. Therefore, it may have broad applications in retina-related

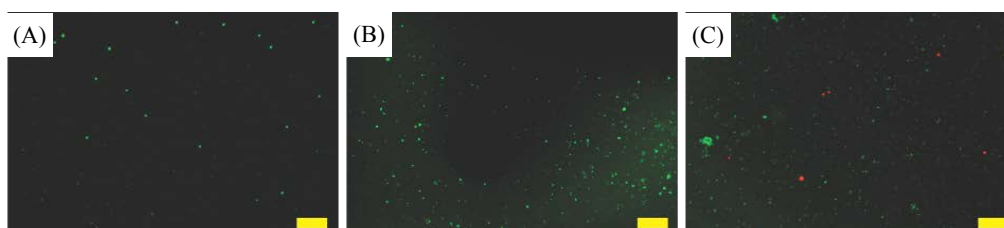


**Figure 8.** Live/dead assay of Y79 cell in bioprinted alginate/pluronic complex bioink at day 1 (A), day 4 (B) and day 7 (C); scale bar: 200  $\mu$ m

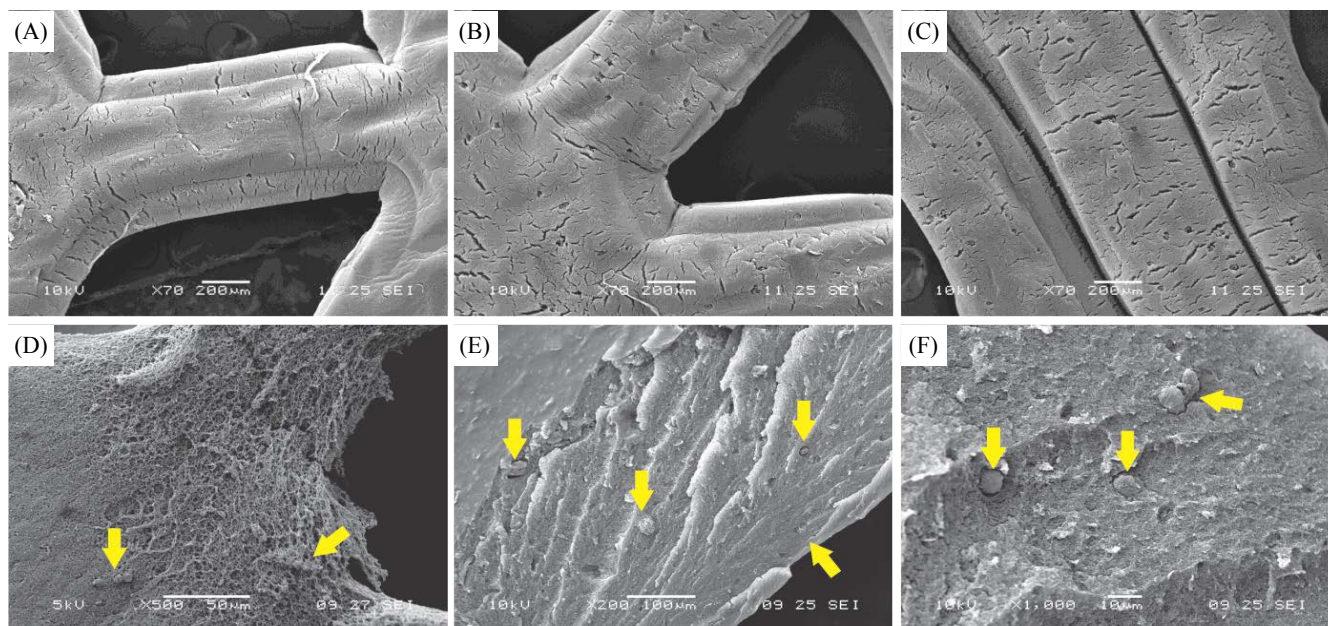


**Figure 9.** SEM images of bioprinted Y79 cell-laden alginate/pluronic complex bioink (A, B and C); Y79 cell distribution at the surface of bioink (D), and the Y79 cell distribution at the cross sections of the alginate/pluronic complex bioink at magnification of 200 $\times$  and 1000 $\times$  (E and F); yellow arrows indicate Y79 cells

research including investigations on disease mechanism, drug testing and treatment methods.

## Conflict of Interest and Funding

No conflict of interest is reported by the authors. The authors wish to thank NTU Start up Grant and NTU-NHG Innovation Collaboration Grant (ARG-14009) for the support.

## References

- Ramsden C M, Powner M B, Carr A J, et al., 2013, Stem cells in retinal regeneration: Past, present and future. *Development*, vol.140(12): 2576–2585.  
<https://dx.doi.org/10.1242/dev.092270>
- Chiba C, 2014, The retinal pigment epithelium: An important player of retinal disorders and regeneration. *Experimental Eye Research*, vol.123: 107–114.  
<https://dx.doi.org/10.1016/j.exer.2013.07.009>
- Aramant R B and Seiler M J, 2004, Progress in retinal sheet transplantation. *Progress in Retinal and Eye Research*, vol. 23(5): 475–494.  
<https://dx.doi.org/10.1016/j.preteyeres.2004.05.003>
- Ghosh F, Juliusson B, Arnér K, et al., 1999, Partial and full-thickness neuroretinal transplants. *Experimental Eye Research*, vol.68(1): 67–74.  
<https://dx.doi.org/10.1006/exer.1998.0582>
- Silverman M S and Hughes S E, 1989, Transplantation of photoreceptors to light-damaged retina. *Investigative Ophthalmology & Visual Science*, vol.30(8): 168–1690.
- Hynes S R and Lavik E B, 2010, A tissue-engineered approach towards retinal repair: Scaffolds for cell transplantation to the subretinal space. *Graefe's Archive for Clinical and Experimental Ophthalmology*, vol.248(6): 763–778.  
<https://dx.doi.org/10.1007/s00417-009-1263-7>
- Li J, Chen M, Fan X, et al., 2016, Recent advances in bioprinting techniques: Approaches, applications and future prospects. *Journal of Translational Medicine*, vol.14: 271.  
<https://dx.doi.org/10.1186/s12967-016-1028-0>
- Fantini M, Curto M, De Crescenzo F, 2016, A method to design biomimetic scaffolds for bone tissue engineering based on Voronoi lattices. *Virtual and Physical Prototyping*, vol.11(2): 77–90.  
<https://dx.doi.org/10.1080/17452759.2016.1172301>
- Cheng K, Mukherjee P, Curthoys I, 2017, Development and use of augmented reality and 3D printing in consulting patient with complex skull base cholesteatoma. *Virtual and Physical Prototyping*, vol.12(3): 241–248.  
<https://dx.doi.org/10.1080/17452759.2017.1310050>
- Zhu W, Ma X, Gou M, et al., 2016, 3D printing of functional biomaterials for tissue engineering. *Current Opinion in Biotechnology*, vol.40: 103–112.  
<https://dx.doi.org/10.1016/j.copbio.2016.03.014>
- Liu H, Zhou H, Lan H, et al., 2017, Organ regeneration: Integration application of cell encapsulation and 3D bioprinting. *Virtual and Physical Prototyping*. In Press.  
<https://dx.doi.org/10.1080/17452759.2017.1338065>
- Zhao X, He J, Xu F, et al., 2016, Electrohydrodynamic printing: A potential tool for high-resolution hydrogel/cell patterning. *Virtual and Physical Prototyping*, vol.11(1): 57–63.  
<https://dx.doi.org/10.1080/17452759.2016.1139378>
- Lorber B, Hsiao W K, Martin K R, 2016, Three-dimensional printing of the retina. *Current Opinion in Ophthalmology*, vol.27(3): 262–267.  
<https://dx.doi.org/10.1097/ICU.0000000000000252>
- Wallace V A, 2011. Concise review: Making a retina—From the building blocks to clinical applications. *Stem Cells*, vol.29(3): 412–417.  
<https://dx.doi.org/10.1002/stem.602>
- Lamba D A, Karl M O, Reh T A, 2009, Strategies for retinal repair: Cell replacement and regeneration. In: Neurotherapy: Progress in Restorative Neuroscience and Neurology, Verhaagen J, et al. (eds), *Progress in Brain Research*, vol.175: 23–31.  
[https://dx.doi.org/10.1016/S0079-6123\(09\)17502-7](https://dx.doi.org/10.1016/S0079-6123(09)17502-7)
- Tan E, Agarwala S, Yap Y L, et al., 2017, Novel method for fabrication ultrathin, free-standing and porous polymer membranes for retinal tissue engineering. *Journal of Materials Chemistry B*. In Press.  
<https://dx.doi.org/10.1039/C7TB00376E>
- Friedman D S, O'Colmain B J, Muñoz B, et al., 2014, Prevalence of age-related macular degeneration in the United States. *Archives of Ophthalmology*, vol.122(4): 564–572.  
<https://dx.doi.org/10.1001/archophth.122.4.564>
- Wong T Y, Loon S C, Saw S M, 2006, The epidemiology of age related eye diseases in Asia. *The British Journal of Ophthalmology*, vol.90(4): 506–511.  
<https://dx.doi.org/10.1136/bjo.2005.083733>
- Schwartz R and Loewenstein A, 2015, Early detection of age related macular degeneration: Current status. *International Journal of Retina and Vitreous*, vol.1(1): 20.  
<https://dx.doi.org/10.1186/s40942-015-0022-7>
- Cheng C L, Saw S M, Pang C E, et al., 2009, Age-related

- macular degeneration in Singapore. *Singapore Medical Journal*, vol.50(2): 126–131.
21. Yeong W Y, Chua C K, Leong K F, *et al.*, 2004, Rapid prototyping in tissue engineering: Challenges and potential. *Trends in Biotechnology*, vol.22(12): 643–652.  
<https://dx.doi.org/10.1016/j.tibtech.2004.10.004>
  22. Chua C K, Yeong W Y, Leong K F, 2005, Rapid prototyping in tissue engineering: A state-of-the-art report. In: *Virtual modeling and rapid manufacturing: Advanced research in virtual and rapid prototyping, Proceedings of the 2nd International Conference on Advanced Research and Rapid Prototyping*; London, UK: Taylor & Francis Group, 19–27.
  23. Mironov V, Zhang J, Gentile C, *et al.*, 2009. Designer ‘blueprint’ for vascular trees: Morphology evolution of vascular tissue constructs. *Virtual and Physical Prototyping*, vol.4(2): 63–74.  
<https://dx.doi.org/10.1080/17452750802657202>
  24. Bártolo P J, Chua C K, Almeida H A, *et al.*, 2009, Biomanufacturing for tissue engineering: Present and future trends. *Virtual and Physical Prototyping*, vol.4(4): 203–216.  
<https://dx.doi.org/10.1080/17452750903476288>
  25. Dalgarno K W, Pallari J H, Woodburn J, *et al.*, 2006, Mass customization of medical devices and implants: State of the art and future directions. *Virtual and Physical Prototyping*, vol.1(3): 137–145.  
<https://dx.doi.org/10.1080/17452750601092031>
  26. Rizzolo L J, 2014, Barrier properties of cultured retinal pigment epithelium. *Experimental Eye Research*, vol.126: 16–26.  
<https://dx.doi.org/10.1016/j.exer.2013.12.018>
  27. Blanch R J, Ahmed Z, Berry M, *et al.*, 2012, Animal models of retinal injury. *Investigative Ophthalmology & Visual Science*, vol.53(6): 2913–2920.  
<https://dx.doi.org/10.1167/iovs.11-8564>
  28. Shi P, Laude A, Yeong W Y, 2017, Investigation of cell viability and morphology in 3D bio-printed alginate constructs with tunable stiffness. *Journal of Biomedical Materials Research Part A*, vol.105(4): 1009–1018.  
<https://dx.doi.org/10.1002/jbm.a.35971>
  29. Yang Y, *et al.*, 2009, A novel mixed micelle gel with thermo-sensitive property for the local delivery of docetaxel. *Journal of Controlled Release*, vol.135(2): 175–182.  
<https://dx.doi.org/10.1016/j.jconrel.2009.01.007>
  30. Jonas J B, Schneider U, Naumann G O H, 1992, Count and density of human retinal photoreceptors. *Graefe's Archive for Clinical and Experimental Ophthalmology*, vol.230(6): 505–510.  
<https://dx.doi.org/10.1007/BF00181769>
  31. Bogenmann E, Lochrie M A, Simon M I, 1988, Cone cell-specific genes expressed in retinoblastoma. *Science*, vol.240(4848): 76–78.  
<https://dx.doi.org/10.1126/science.2451289>
  32. Di Polo A and Farber D B, 1995, Rod photoreceptor-specific gene expression in human retinoblastoma cells. *Proceedings of the National Academy of Sciences of the United States*, vol.92(9): 4016–4020.  
<https://dx.doi.org/10.1073/pnas.92.9.4016>
  33. Wiechmann A F, 1996, Recoverin in cultured human retinoblastoma cells: Enhanced expression during morphological differentiation. *Journal of Neurochemistry*, vol.67(1): 105–110.  
<https://dx.doi.org/10.1046/j.1471-4159.1996.67010105.x>
  34. Messmer E P, Font R L, Kirkpatrick J B, *et al.*, 1985, Immunohistochemical demonstration of neuronal and astrocytic differentiation in retinoblastoma. *Ophthalmology*, vol.92(1): 167–173.  
[https://dx.doi.org/10.1016/S0161-6420\(85\)34076-9](https://dx.doi.org/10.1016/S0161-6420(85)34076-9)
  35. Tan E, Ding X Q, Saadi A, *et al.*, 2004, Expression of cone-photoreceptor-specific antigens in a cell line derived from retinal tumors in transgenic mice. *Investigative Ophthalmology & Visual Science*, vol.45(3): 764–768.  
<https://dx.doi.org/10.1167/iovs.03-1114>